

The Color Dipole Picture of low-x DIS

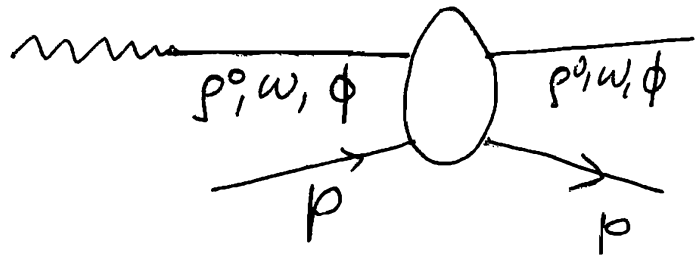
Dieter Schildknecht

Universität Bielefeld & Max Planck Institut für Physik, München

Ringberg Workshop on New Trends in HERA Physics,
September 25 – 28, 2011

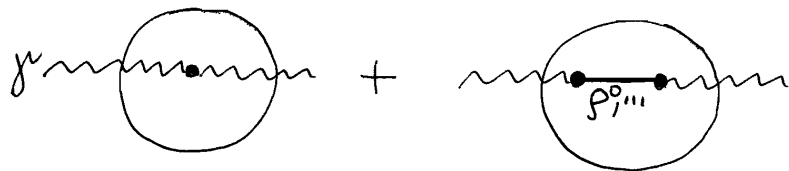
1. Introduction

1960's Vector Meson Dominance



J.J. Sakurai (1960, ...)

Shadowing in γA interactions



Leo Stodolsky (1967)

1969 DIS SLAC-MIT Collaboration

Bjorken scaling,
parton model

Volume 40B, number 1

PHYSICS LETTERS

12 June 1972

GENERALIZED VECTOR DOMINANCE AND INELASTIC ELECTRON-PROTON SCATTERING *

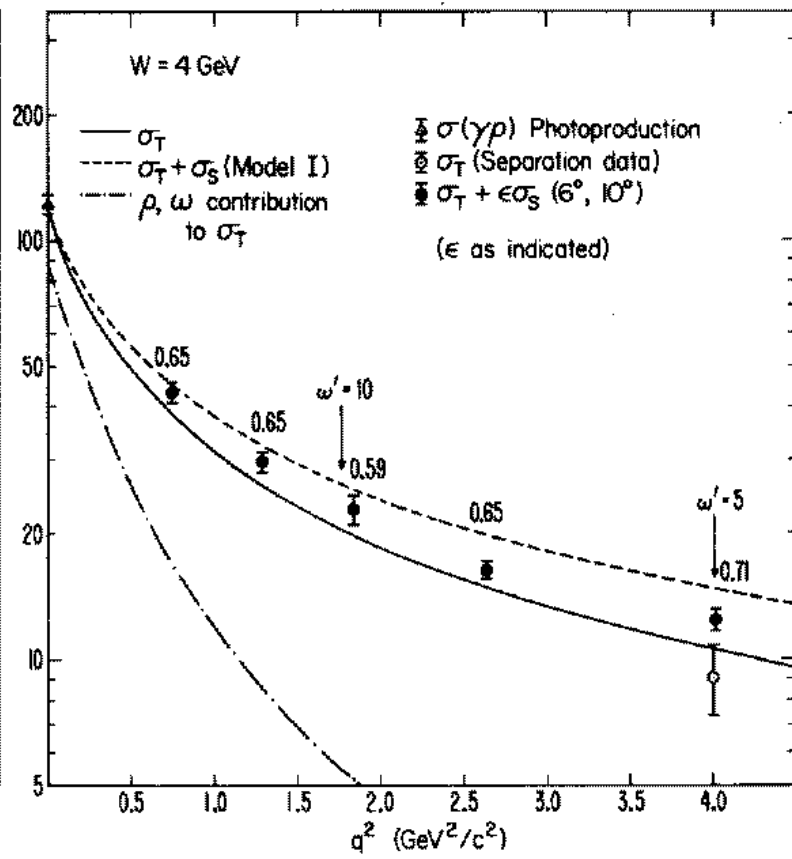
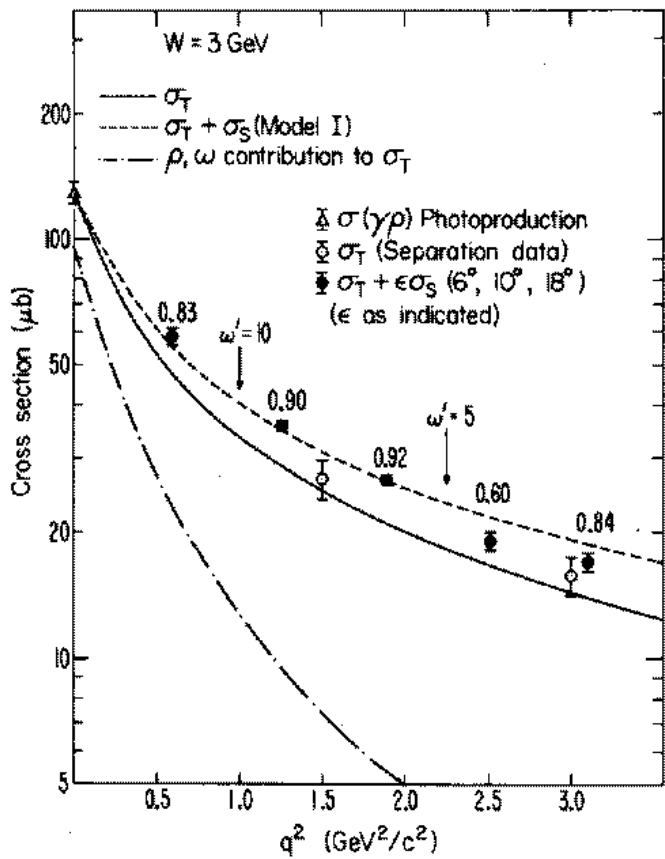
J. J. SAKURAI and D. SCHILDKNECHT **
*Department of Physics, University of California,
Los Angeles, USA*

Received 30 March 1972

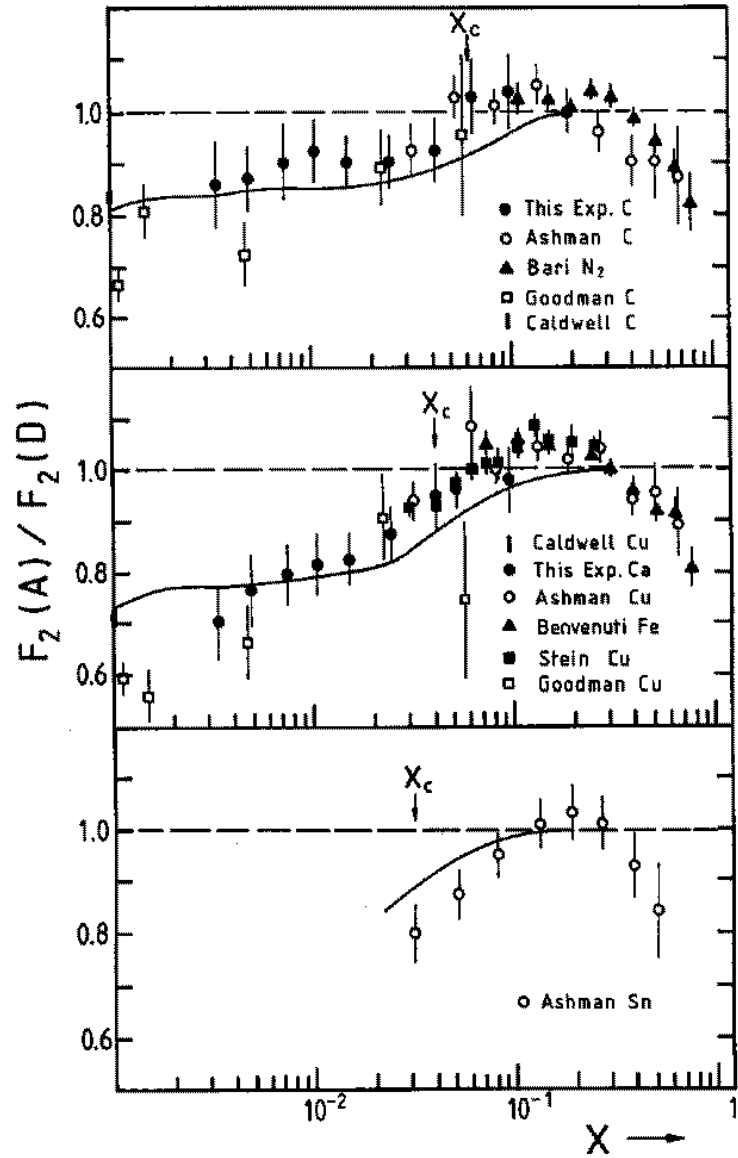
* We propose a model of inelastic electron-proton scattering which takes into account the coupling of the photon to higher-mass vector states. Both the virtual photon-proton cross section σ_T (predicted with essentially no adjustable parameters) and the q^2 dependence of R are in exceedingly good agreement with the SLAC-MIT data in the diffraction region.

$$\gamma \text{ wavy line} \xrightarrow{p^0, \omega, \phi} + \gamma \text{ wavy line} \xrightarrow{\text{massive continuum}}$$

(1972)



1989 Shadowing EMC Collaboration



D. Schildknecht (1973)

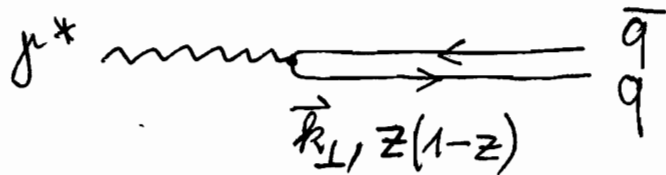
C. Bilchak and D. Schildknecht (1989)

1994 HERA

DIS for $x_{bj} \ll 0.1$, High-mass diffractive production
("rap-gap" events) at HERA

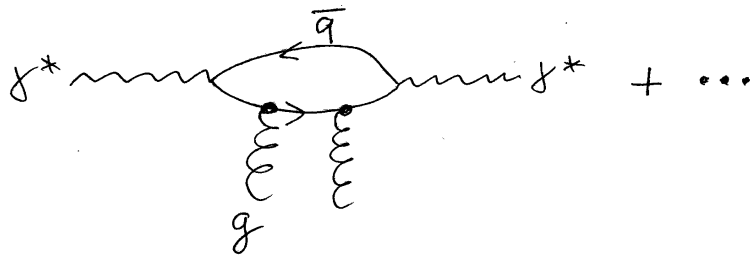
Modern picture of low-x DIS:

i) $q\bar{q}$ internal structure



Nikolaev, Zakharov (1991)

ii) $q\bar{q}$ -dipole interaction

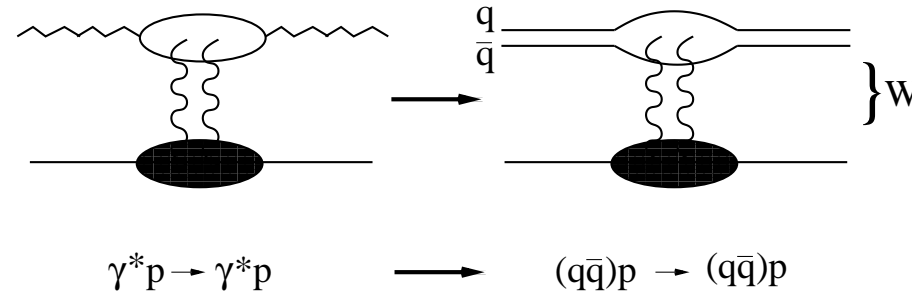


Low (1975)

Nussinov (1975)

2. The CDP: Model-independent Results.

The longitudinal and the transverse photoabsorption cross section



$$A) \quad \sigma_{\gamma_{L,T}^*}(W^2, Q^2) = \int dz \int d^2\vec{r}_\perp |\psi_{L,T}(\vec{r}_\perp, z(1-z), Q^2)|^2 \sigma_{(q\bar{q})p}(\vec{r}_\perp, z(1-z), W^2)$$

Remarks: i) $|\psi_{L,T}(\vec{r}_\perp, z(1-z), Q^2)|$: Probability for $\gamma_{L,T}^* \rightarrow q\bar{q}$ fluctuation

ii) $\sigma_{(q\bar{q})p}(\vec{r}_\perp, z(1-z), W^2)$: $(q\bar{q})p$ cross section dependent on W^2 (not on $x \equiv \frac{Q^2}{W^2}$)

Lifetime of $q\bar{q}$ fluctuation:

$$\frac{1}{\Delta E} = \frac{2\nu}{Q^2 + M_{q\bar{q}}^2} = \frac{1}{x + \frac{M_{q\bar{q}}^2}{W^2}} \frac{1}{M_p} \gg \frac{1}{M_p}, \quad \begin{array}{l} Q^2 \equiv -q^2 \geq 0 \\ x < 0.1 \end{array}$$

B) Gauge-invariant two-gluon coupling:

$$\begin{aligned}\sigma_{(q\bar{q})p}(\vec{r}_\perp, z(1-z), W^2) &= \int d^2\vec{l}_\perp \tilde{\sigma}(\vec{l}_\perp^2, z(1-z), W^2) \left(1 - e^{-i\vec{l}_\perp \cdot \vec{r}_\perp}\right) \\ &\cong \frac{\pi}{4} \vec{r}_\perp^2 \int d\vec{l}_\perp^2 \vec{l}_\perp^2 \tilde{\sigma}(\vec{l}_\perp^2, z(1-z), W^2).\end{aligned}$$

Nikolaev, Zakharov (1991)

“color transparency” for

$$\vec{r}_\perp^2 \vec{l}_\perp^2 < \vec{r}_\perp^2 \vec{l}_\perp^2_{Max}(W^2) < 1$$

$\sigma_{\gamma_{L,T}^*}(W^2, Q^2)$ for large Q^2

$$|\psi_{L,T}(\mathbf{r}_\perp, z(1-z), Q^2)|^2 \sim K_{0,1}^2(\underbrace{r_\perp \sqrt{z(1-z)} \sqrt{Q^2}}_{\equiv r'_\perp Q}) \sim \frac{1}{r'_\perp Q} e^{-2r'_\perp Q} \quad \text{for } r'_\perp Q \gg 1.$$

Dominant contribution from $r'_\perp Q^2 < 1$.

For $l'^2_{\perp \text{Max}}(W^2) < Q^2$,

$$r'^2_{\perp \text{Max}}(W^2) = r^2_{\perp \text{Max}}(W^2) < 1. \quad \left(\vec{l}'^2_{\perp} = \frac{l^2_{\perp}}{z(1-z)} \right)$$

Color transparency, $\sigma_{(q\bar{q})p} \sim r^2_{\perp}$.

Using $\int dy y^3 K_0^2(y) = \frac{1}{3}$,

$$\int dy y^3 K_1^2(y) = \frac{2}{3},$$

$$\sigma_{\gamma_{L,T}^*}(W^2, Q^2) = \alpha \sum Q_q^2 \frac{1}{Q^2} \int dz \int d\vec{l}'^2_{\perp} \vec{l}'^2_{\perp} \tilde{\sigma}(\vec{l}'^2_{\perp}, z(1-z), W^2) \begin{cases} 1, \\ 2\rho_W. \end{cases}$$

Substitution rule: $\sigma_{\gamma_L^* p}(W^2, Q^2) \rightarrow \sigma_{\gamma_T^* p}(W^2, Q^2)$

via: $K_0^2(r'_\perp Q) \rightarrow K_1^2(r'_\perp Q),$
 $\sigma_{(q\bar{q})p}(\vec{r}'_\perp{}^2, \dots) \rightarrow \sigma_{(q\bar{q})p}(\rho_W \vec{r}'_\perp{}^2, \dots)$

Transverse-size enhancement (for $\rho_W > 1$):

$$(\gamma_L^* \rightarrow q\bar{q}) \rightarrow (\gamma_T^* \rightarrow q\bar{q})$$

$$R(W^2, Q^2) \equiv \frac{\sigma_{\gamma_L^* p}(W^2, Q^2)}{\sigma_{\gamma_T^* p}(W^2, Q^2)} = \frac{1}{2\rho_W}$$

$(q\bar{q})_{L,T}^{J=1}$ states : $\gamma_{L,T}^* \rightarrow (q\bar{q})_{L,T}^{J=1}$

$$\sigma_{\gamma_{L,T}^* p}(W^2, Q^2) = \alpha \sum_q Q_q^2 \frac{1}{Q^2} \frac{1}{6} \left\{ \begin{array}{l} \int d\vec{l}_\perp'^2 \vec{l}_\perp'^2 \bar{\sigma}_{(q\bar{q})_{L=1} p}(\vec{l}_\perp'^2, W^2), \\ 2 \int d\vec{l}_\perp'^2 \vec{l}_\perp'^2 \bar{\sigma}_{(q\bar{q})_{T=1} p}(\vec{l}_\perp'^2, W^2). \end{array} \right.$$

$$\rho_W = \frac{\int d\vec{l}_\perp'^2 \vec{l}_\perp'^2 \bar{\sigma}_{(q\bar{q})_{T=1} p}(\vec{l}_\perp'^2, W^2)}{\int d\vec{l}_\perp'^2 \vec{l}_\perp'^2 \bar{\sigma}_{(q\bar{q})_{L=1} p}(\vec{l}_\perp'^2, W^2)}.$$

Numerical value of $\rho_W = \rho$:

$$\vec{l}_\perp^2 = z(1-z)\vec{l}_\perp'^2$$

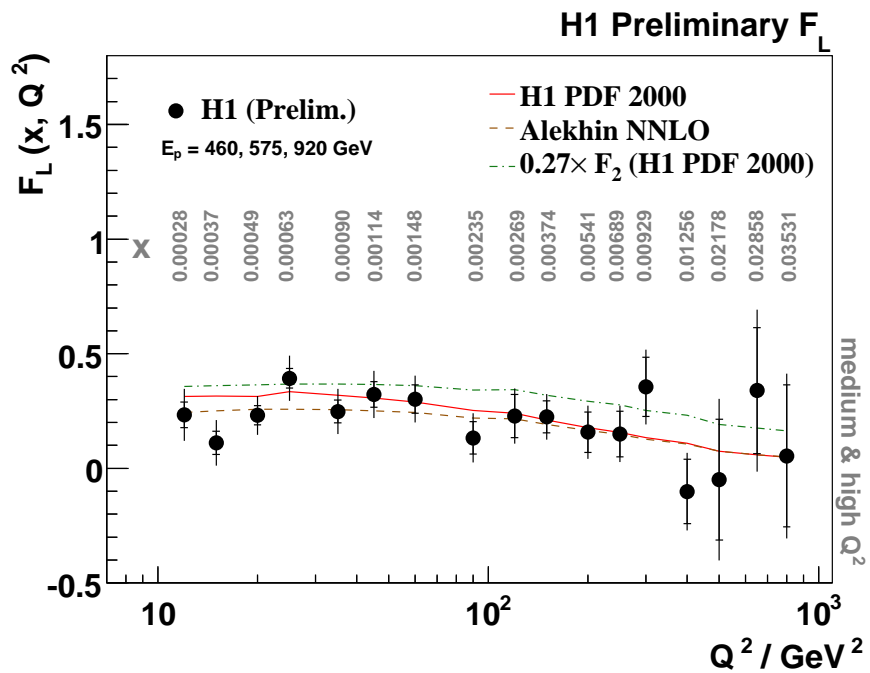
$$\langle \vec{l}_\perp^2 \rangle_{L,T}^{\vec{l}_\perp'^2 = \text{const}} = \vec{l}_\perp'^2 \left\{ \begin{array}{l} 6 \int dz z^2 (1-z)^2 = \frac{4}{20} \vec{l}_\perp'^2, \\ \frac{3}{2} \int dz z(1-z)(1-2z(1-z)) = \frac{3}{20} \vec{l}_\perp'^2. \end{array} \right.$$

Uncertainty principle:

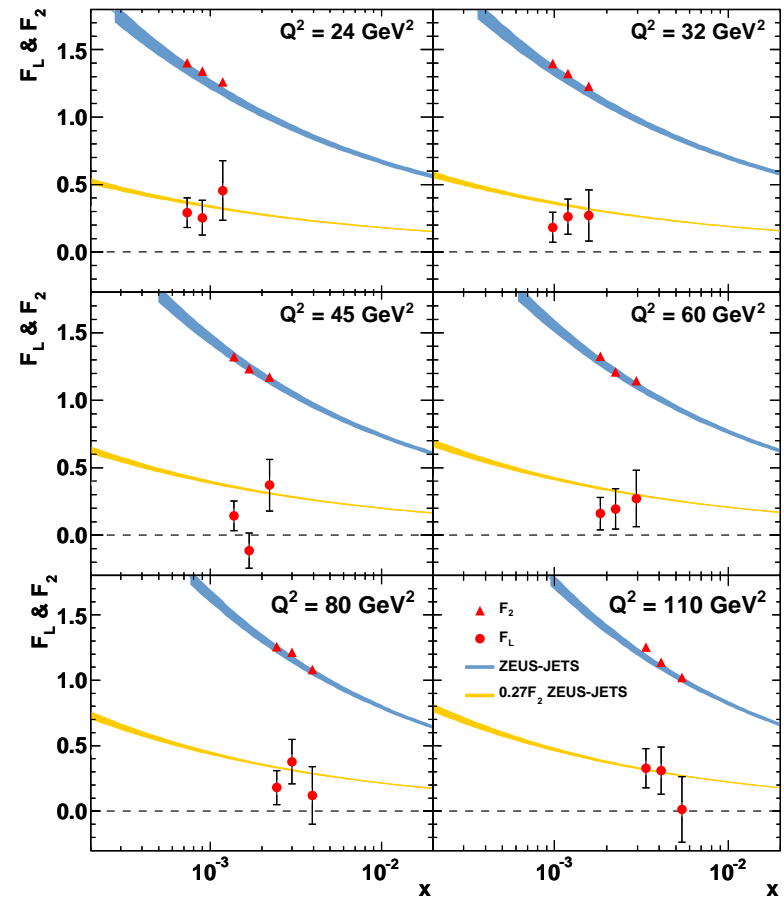
$$\rho_W = \frac{\langle r_\perp^2 \rangle_T}{\langle \vec{r}_\perp^2 \rangle_L} = \frac{\langle \vec{l}_\perp^2 \rangle_L}{\langle \vec{l}_\perp^2 \rangle_T} = \frac{4}{3} \equiv \rho.$$

$$R = \frac{1}{2\rho} = \begin{cases} 0.5 \text{ for } \rho = 1, \\ \frac{3}{8} = 0.375 \text{ for } \rho = \frac{4}{3}. \end{cases} \quad \text{ad hoc, helicity independence}$$

Kuroda, Schildknecht (2008)

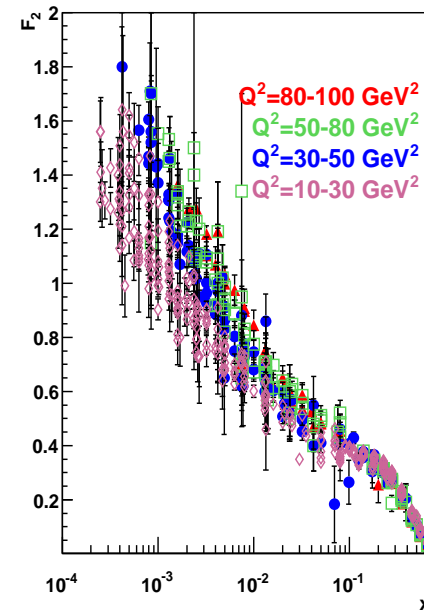
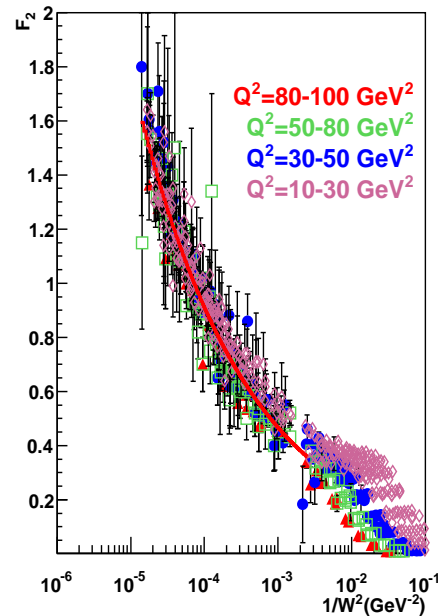


ZEUS



The W-dependence

$$\begin{aligned} F_2(x, Q^2) &\cong \frac{Q^2}{4\pi^2\alpha} \left(\sigma_{\gamma_{LP}^*}(W^2, Q^2) + \sigma_{\gamma_{TP}^*}(W^2, Q^2) \right) \\ &= \frac{\sum_q Q_q^2}{4\pi^2} \int dz \int d\vec{l}_\perp^2 \tilde{\sigma}(\vec{l}_\perp^2, z(1-z), W^2)(1+2\rho). \end{aligned}$$



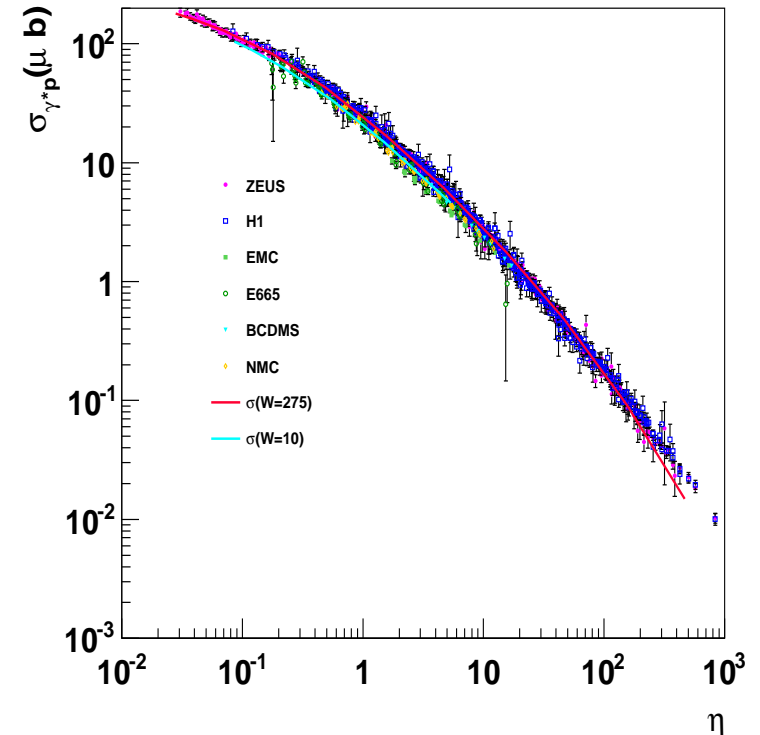
Prabhdeep Kaur (2010)

Low-x Scaling

Empirically :

$$\eta \equiv \frac{Q^2 + m_0^2}{\Lambda_{sat}^2(W^2)},$$

$$\Lambda_{sat}^2(W^2) \sim (W^2)^{C_2}$$



Schildknecht, Surrow, Tentyukov (2000)

$$\sigma_{\gamma^*p}(W^2, Q^2) = \sigma_{\gamma^*p}(\eta(W^2, Q^2))$$

$$\sim \sigma^{(\infty)} \begin{cases} \ln \frac{1}{\eta(W^2, Q^2)} & , \text{ for } \eta(W^2, Q^2) \ll 1 \\ \frac{1}{\eta(W^2, Q^2)} & , \text{ for } \eta(W^2, Q^2) \gg 1 \end{cases}$$

Low-x scaling: Direct consequence of CDP

$$\begin{aligned}\sigma_{(q\bar{q})_{L,T}^{J=1}p}(\vec{r}'_{\perp}, W^2) &= \int d^2\vec{l}'_{\perp} \bar{\sigma}_{(q\bar{q})_{L,T}^{J=1}p}(\vec{l}'_{\perp}, W^2) (1 - e^{-i\vec{l}'_{\perp} \cdot \vec{r}'_{\perp}}) \\ &= \pi \int d^2\vec{l}'_{\perp} \bar{\sigma}_{(q\bar{q})_{L,T}^{J=1}p}(\vec{l}'_{\perp}, W^2) \cdot \underbrace{\left(1 - \frac{\int d^2\vec{l}'_{\perp} \bar{\sigma}_{(q\bar{q})_{L,T}^{J=1}p}(\vec{l}'_{\perp}, W^2) J_0(l'_{\perp} r'_{\perp})}{\int d^2\vec{l}'_{\perp} \bar{\sigma}_{(q\bar{q})_{L,T}^{J=1}p}(\vec{l}'_{\perp}, W^2)}\right)}\end{aligned}$$

i) “1 - 1” destructive interference
color transparency

$$r'_{\perp}{}^2 < \frac{1}{l'_{\perp \text{ Max}}(W^2)}$$

$$J_0(l'_{\perp} r'_{\perp}) \cong 1 - \frac{1}{4}(l'_{\perp} r'_{\perp})^2 + \dots$$

ii) “1-0=1” hadronlike “saturation”

$$\frac{1}{l'_{\perp \text{ Max}}(W^2)} < r'_{\perp}{}^2$$

$$\begin{aligned}\sigma_{(q\bar{q})_{L,T}^{J=1}p}(r'_{\perp}{}^2, W^2) &\cong \pi \int d^2\vec{l}'_{\perp} \bar{\sigma}_{(q\bar{q})_{L,T}^{J=1}p}(\vec{l}'_{\perp}, W^2) \\ &\equiv \sigma_{L,T}^{(\infty)}(W^2)\end{aligned}$$

Note: a) $r'_{\perp}{}^2$ fixed, $W^2 \rightarrow \infty$,

b) $r'_{\perp}{}^2 \rightarrow \infty$, W^2 fixed

$$\sigma_{\gamma^*p}(W^2, Q^2) \sim \begin{cases} \sigma^{(\infty)} \frac{\Lambda_{sat}^2(W^2)}{Q^2} \sim \frac{\sigma^{(\infty)}}{\eta(W^2, Q^2)} & , \quad \eta(W^2, Q^2) \gg 1 & (i) \\ \sigma^{(\infty)} \ln \frac{1}{\eta(W^2, Q^2)} & , \quad \eta(W^2, Q^2) \ll 1 & (ii) \end{cases}$$

Direct consequence of CDP, NOT dependent on a specific parameterization dipole cross section.

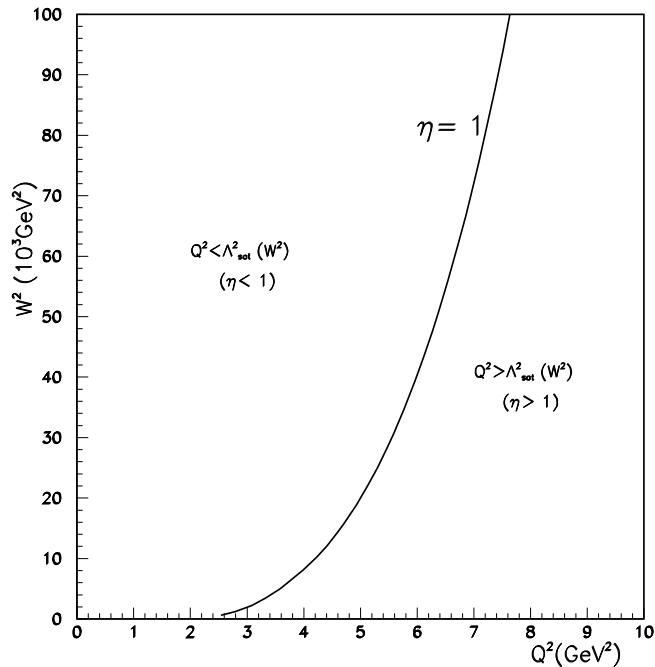
$$\begin{aligned} \Lambda_{sat}^2(W^2) &\equiv \frac{\int d\vec{l}'_{\perp} \vec{l}'_{\perp} \bar{\sigma}_{(q\bar{q})_L^{J=1p}}(\vec{l}'_{\perp}, W^2)}{\int d\vec{l}'_{\perp} \bar{\sigma}_{(q\bar{q})_L^{J=1p}}(\vec{l}'_{\perp}, W^2)} \\ &= \frac{1}{\sigma_L^{(\infty)}(W^2)} \pi \cdot \int d\vec{l}'_{\perp} \vec{l}'_{\perp} \bar{\sigma}_{(q\bar{q})_L^{J=1p}}(\vec{l}'_{\perp}, W^2) \end{aligned}$$

The limit of $\eta(W^2, Q^2) \rightarrow 0$, or $W^2 \rightarrow \infty$ at Q^2 fixed

$$\lim_{\substack{W^2 \rightarrow \infty \\ Q^2 \text{ fixed}}} \frac{\sigma_{\gamma^*p}(\eta(W^2, Q^2))}{\sigma_{\gamma^*p}(\eta(W^2, Q^2 = 0))} = \lim_{\substack{W^2 \rightarrow \infty \\ Q^2 \text{ fixed}}} \frac{\ln \left(\frac{\Lambda_{sat}^2(W^2)}{m_0^2} \frac{m_0^2}{(Q^2 + m_0^2)} \right)}{\ln \frac{\Lambda_{sat}^2(W^2)}{m_0^2}} = 1 + \lim_{\substack{W^2 \rightarrow \infty \\ Q^2 \text{ fixed}}} \frac{\ln \frac{m_0^2}{Q^2 + m_0^2}}{\ln \frac{\Lambda_{sat}^2(W^2)}{m_0^2}} = 1.$$

$$\sigma_{\gamma^*p}(\eta(W^2, Q^2 = 0)) = \sigma_{\gamma p}(W^2)$$

D. Schildknecht, DIS 2001 (Bologna)



$Q^2 [GeV^2]$	$W^2 [GeV^2]$	$\frac{\sigma_{\gamma^*p}(\eta(W^2, Q^2))}{\sigma_{\gamma p}(W^2)}$
1.5	2.5×10^7	0.5
	1.26×10^{11}	0.63

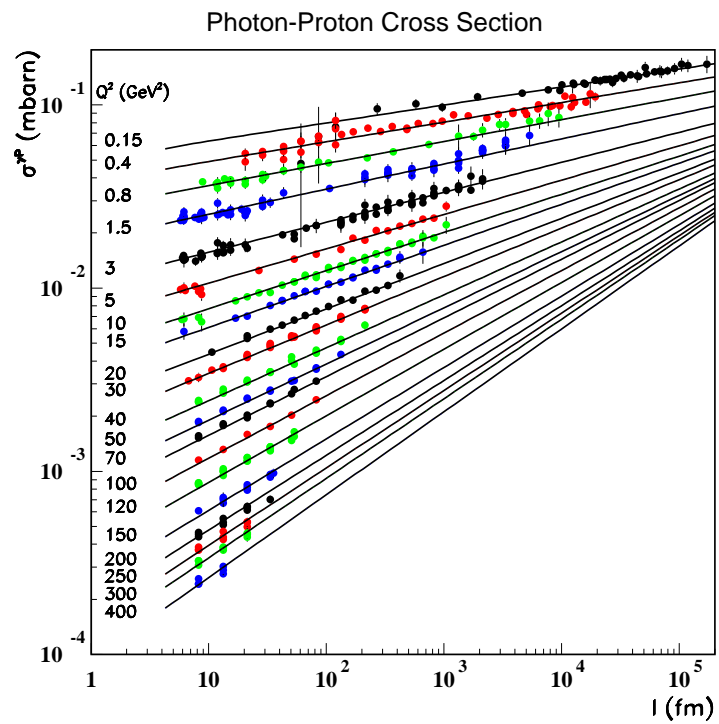
Observation by Caldwell

$$\sigma_{\gamma^*p}(W^2, Q^2) = \sigma_0(Q^2) \left(\frac{1}{2M_p} \frac{W^2}{Q^2} \right)^{\lambda_{eff}(Q^2)}$$

A. Caldwell (2008)

Q^2 -independent limit at approximately

$$W^2 \simeq 10^9 Q^2.$$



Summarizing this Section on model-independent results:

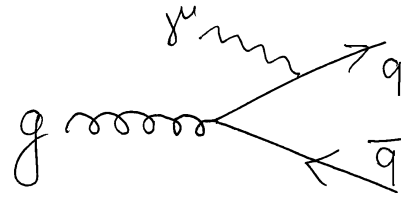
$$R = \frac{1}{2\rho} = \frac{3}{8};$$

$$\text{Low - x scaling : } \sigma_{\gamma^*p} \sim \sigma^{(\infty)} \begin{cases} \frac{1}{\eta(W^2, Q^2)} & , \quad \eta(W^2, Q^2) > 1, \\ \ln \frac{1}{\eta(W^2, Q^2)} & , \quad \eta(W^2, Q^2) < 1. \end{cases}$$

$$W^2 \rightarrow \infty,$$

Q^2 fixed : Q^2 – independent limit coinciding with $Q^2 = 0$ photoproduction, $\sigma_{\gamma p}(W^2)$.

3. The CDP, the Gluon Distribution Function and Evolution.



CDP ↔ Photon-Gluon Fusion of pQCD

$$F_L(x, Q^2) = \frac{\alpha_s(Q^2)}{3\pi} \sum_q Q_q^2 \cdot 6I_g(x, Q^2),$$

where $I_g(x, Q^2) \equiv \int_x^1 \frac{dy}{y} \left(\frac{x}{y}\right)^2 \left(1 - \frac{x}{y}\right) yg(y, Q^2)$.

$$F_L(\xi_L x, Q^2) = \frac{\alpha_s(Q^2)}{3\pi} \sum_q Q_q^2 G(x, Q^2).$$

Cooper-Sarkar et al. (1988)

$$F_2(x, Q^2) = \frac{5}{18} x \sum(x, Q^2).$$

$$\frac{\partial F_2(\xi_2 x, Q^2)}{\partial \ln Q^2} = \frac{\alpha_s(Q^2)}{3\pi} \sum_q Q_q^2 G(x, Q^2).$$

rescaling factors:

$$(\xi_L, \xi_2) \simeq (0.40, 0.50)$$

$$(\xi_L, \xi_2) = (0.45, 0.40) \text{ for specific}$$

gluon distribution.

Accuracy $\lesssim 0.5\%$.

Prytz (1993)

Using $F_L(x, Q^2) = \frac{1}{2\rho+1}F_2(x, Q^2)$:

$$(2\rho + 1)\frac{\partial}{\partial \ln Q^2}F_2\left(\frac{\xi_2}{\xi_L}x, Q^2\right) = F_2(x, Q^2)$$

i) CDP: $F_2(x, Q^2) = F_2(W^2)$:

$$(2\rho_W + 1)\frac{\partial}{\partial \ln W^2}F_2\left(\frac{\xi_L}{\xi_2}W^2\right) = F_2(W^2)$$

ii) Power law

$$F_2(W^2) \sim (W^2)^{C_2} = \left(\frac{Q^2}{x}\right)^{C_2}$$

Compare: “hard Pomeron” solution of DGLAP evolution: $\left(\frac{1}{x}\right)^{\lambda = \text{fixed}}$.

“hard Pomeron” Regge: $\left(\frac{1}{x}\right)^{\epsilon_0 \simeq 0.43}$

$$(2\rho_W + 1)C_2 \left(\frac{\xi_L}{\xi_2}\right)^{C_2} = 1$$

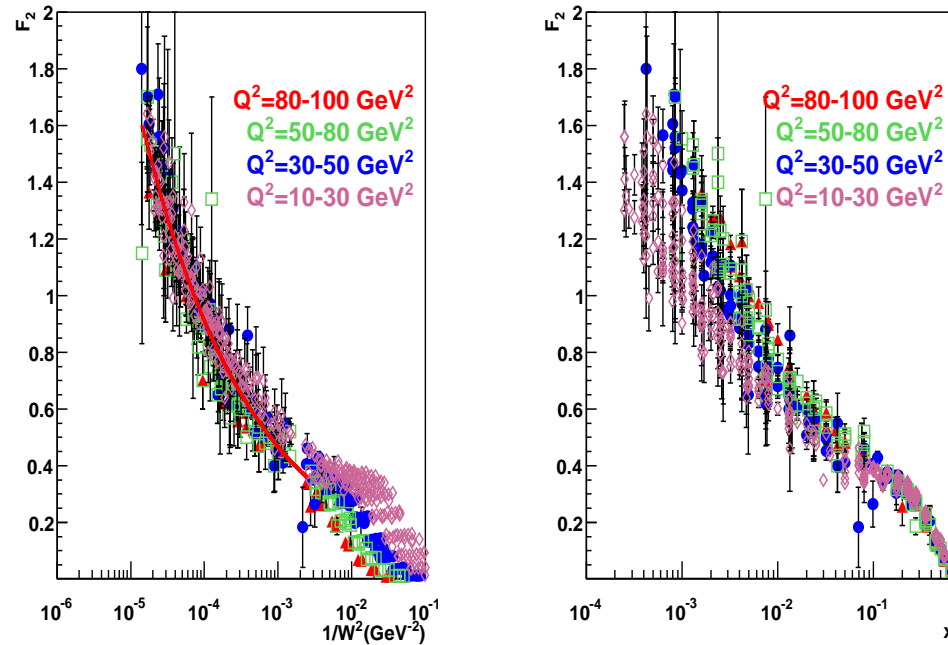
with $\rho = \frac{4}{3}$,

$$C_2 = \frac{1}{2\rho+1} \left(\frac{\xi_2}{\xi_L}\right)^{C_2} = 0.29$$

Kuroda, Schildknecht (2011)

$$F_2(W^2) = f_2 \cdot \left(\frac{W^2}{1\text{GeV}^2} \right)^{C_2=0.29}$$

$f_2 = 0.063$ (fitted parameter)



Experimental evidence for $F_2(x, Q^2) = F_2(W^2 \cong Q^2/x)$
and for the prediction of $C_2 = 0.29$.

The Gluon Distribution Function

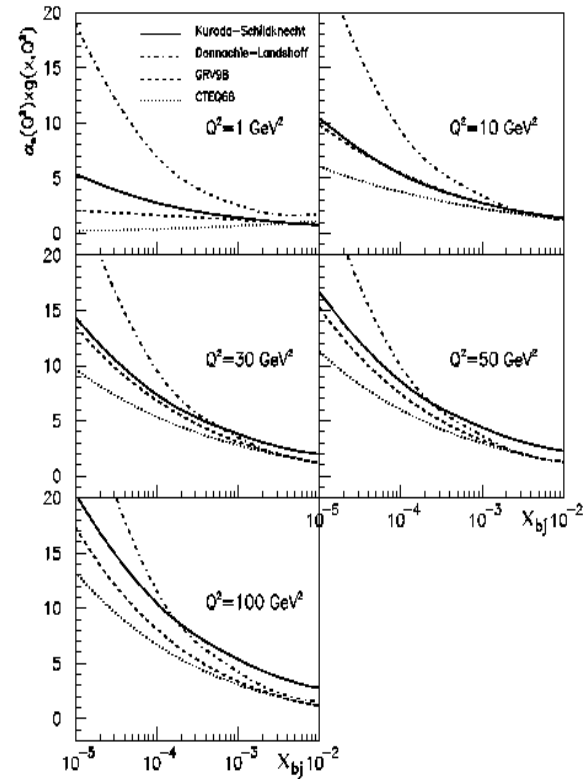
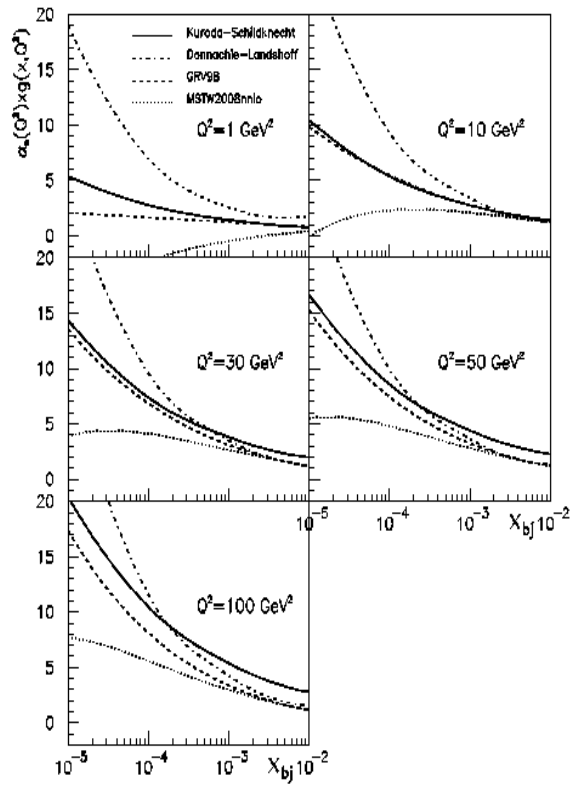
$$\begin{aligned}\alpha_s(Q^2)G(x, Q^2) &= \frac{3\pi}{\sum_q Q_q^2} F_L(\xi_L x, Q^2) \\ &= \frac{3\pi}{\sum_q Q_q^2} \frac{1}{(2\rho + 1)} F_2(\xi_L x, Q^2) \\ &= \frac{3\pi}{\sum_q Q_q^2 (2\rho + 1)} \frac{f_2}{\xi_L^{C_2=0.29}} \left(\frac{W^2}{1\text{GeV}^2} \right)^{C_2=0.29}\end{aligned}$$

Comments:

$$\begin{aligned}\text{CDP: } F_{L,2} &= F_{L,2} \left(W^2 = \frac{Q^2}{x} \right), \\ \rho &= \text{const.} = \frac{4}{3},\end{aligned}$$

$C_2 = 0.29$ from evolution

$f_2 = 0.063$ fit parameter



Comparison with gluon distributions from Durham data file using $\alpha_s(Q^2) = \alpha_s(Q^2)^{NLO}$

4. Models for the Dipole Cross Section

Cvetic, Schildknecht,
Surrow, Tentyukov (2001)

Model-independently:

$$\sigma_{\gamma^*p} \sim \begin{cases} \ln \frac{1}{\eta(W^2, Q^2)} & , \quad \eta(W^2, Q^2) \ll 1 \\ \frac{1}{\eta(W^2, Q^2)} & , \quad \eta(W^2, Q^2) \gg 1 \end{cases}$$

Detailed ansatz for dipole cross section: Interpolation between $\eta(W^2, Q^2) < 1$ and $\eta(W^2, Q^2) > 1$.

Simple ansatz with $\rho = 1$, $\left(R = \frac{1}{2\rho} = \frac{1}{2}\right)$:

$$\sigma_{(q\bar{q})p}(\vec{r}_\perp, z(1-z), W^2) = \sigma^{(\infty)}(W^2) \left(1 - J_0\left(r_\perp \sqrt{z(1-z)} \Lambda_{sat}(W^2)\right)\right)$$

$$\begin{aligned} \sigma_{\gamma^*p}(W^2, Q^2) &= \sigma_{\gamma^*p}(\eta(W^2, Q^2)) + O\left(\frac{m_0^2}{\Lambda_{sat}^2(W^2)}\right) = \\ &= \frac{\alpha R_{e^+e^-}}{3\pi} \sigma^{(\infty)}(W^2) I_0(\eta) + O\left(\frac{m_0^2}{\Lambda_{sat}^2(W^2)}\right), \quad R_{e^+e^-} = 3 \sum_q Q_q^2. \end{aligned}$$

$$\begin{aligned} I_0(\eta(W^2, Q^2)) &= \frac{1}{\sqrt{1 + 4\eta(W^2, Q^2)}} \ln \frac{\sqrt{1 + 4\eta(W^2, Q^2)} + 1}{\sqrt{1 + 4\eta(W^2, Q^2)} - 1} \cong \\ &\cong \begin{cases} \ln \frac{1}{\eta(W^2, Q^2)} + O(\eta \ln \eta), & \text{for } \eta(W^2, Q^2) \rightarrow \frac{m_0^2}{\Lambda_{sat}^2(W^2)}, \\ \frac{1}{2\eta(W^2, Q^2)} + O\left(\frac{1}{\eta^2}\right), & \text{for } \eta(W^2, Q^2) \rightarrow \infty, \end{cases} \end{aligned}$$

Generalization to $\rho = \frac{4}{3}$.

Constraint: $m_0^2 \leq M_{q\bar{q}}^2, M'_{q\bar{q}} \leq m_1^2(W^2)$;

Kuroda, Schildknecht (2011)

$$\sigma_{\gamma^*p} = \sigma_{\gamma^*p} \left(\eta(W^2, Q^2), \frac{m_0^2}{\Lambda_{sat}^2(W^2)}, \xi \equiv \frac{m_1^2(W^2)}{\Lambda_{sat}^2(W^2)} \right),$$

$$\eta(W^2, Q^2) = \frac{Q^2 + m_0^2}{\Lambda_{sat}^2(W^2)},$$

$$\Lambda_{sat}^2(W^2) = C_1 \left(\frac{W^2}{W_0^2} + 1 \right)^{C_2} \cong \text{const} \left(\frac{W^2}{1\text{GeV}^2} \right)^{C_2}$$

$$C_1 = 1.95\text{GeV}^2$$

$$W_0^2 = 1081\text{GeV}^2$$

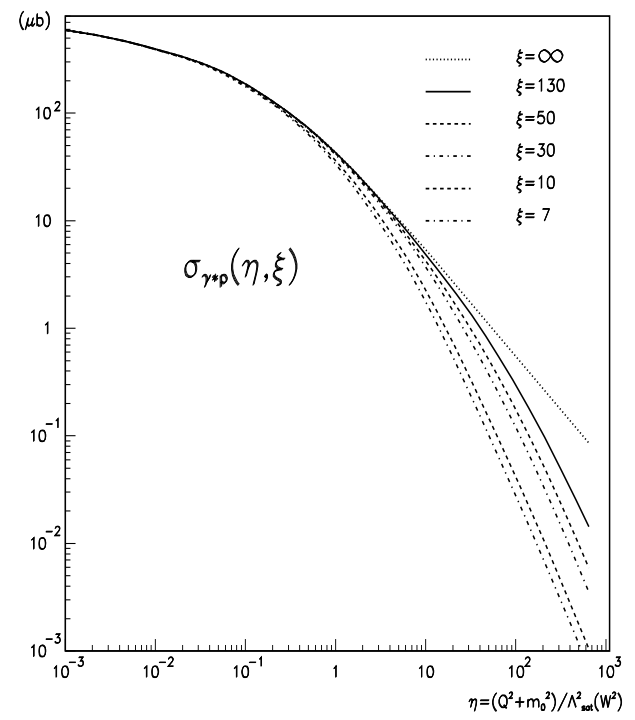
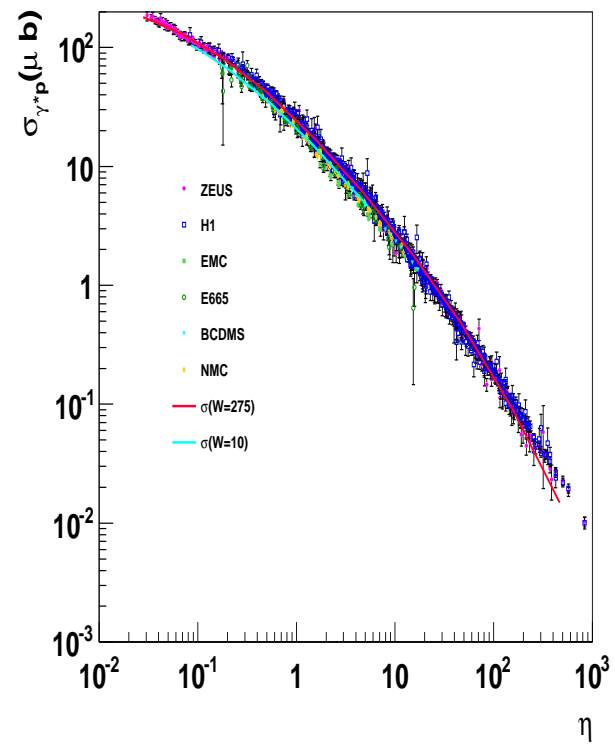
$$C_2 = 0.27(0.29)$$

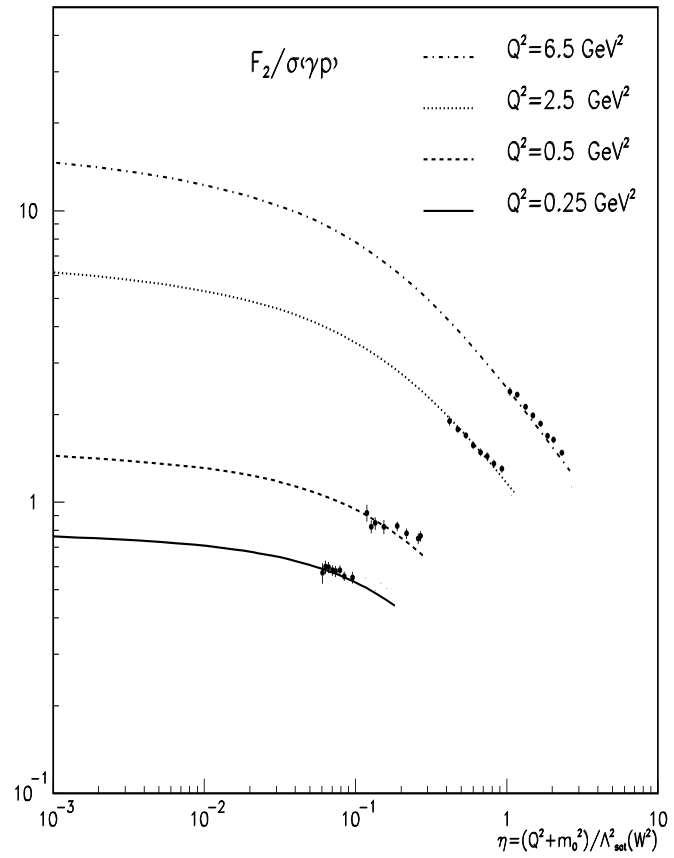
$$m_0^2 = 0.15\text{GeV}^2$$

$$m_1^2(W^2) = \xi \Lambda_{sat}^2(W^2) = 130 \Lambda_{sat}^2(W^2)$$

Normalization by $Q^2 = 0$ photoproduction (Regge fit):

$$\sigma^{(\infty)}(W^2) \cong \begin{cases} 30\text{mb}, & (\text{for 3 active flavors, } R_{e^+e^-} = 2) \\ 18\text{mb}, & (\text{for 4 active flavors, } R_{e^+e^-} = \frac{10}{3}) \end{cases}$$



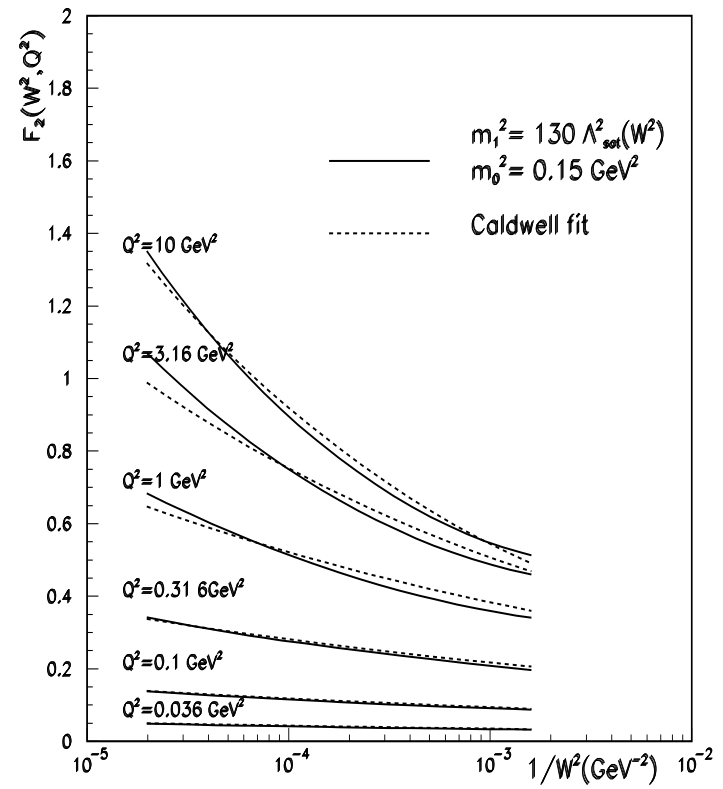
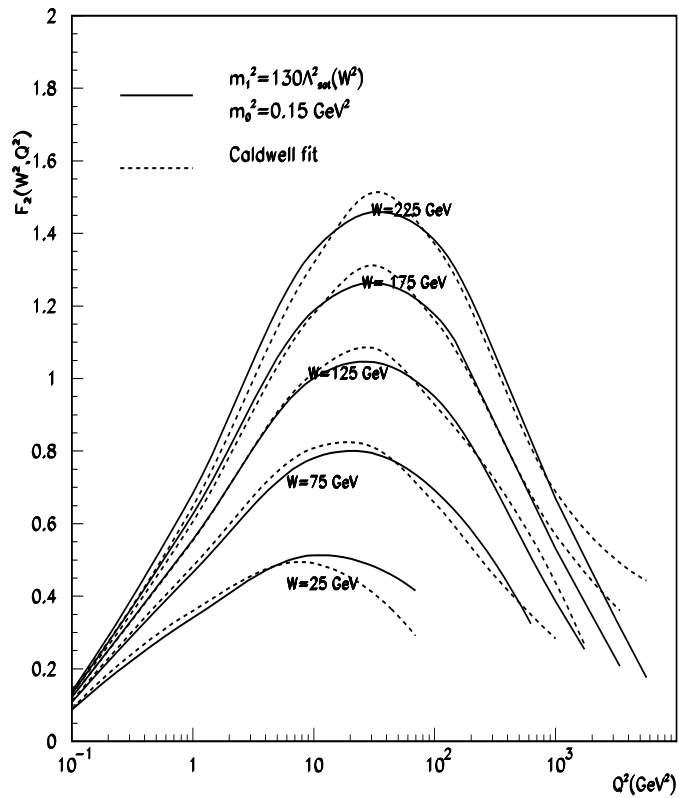


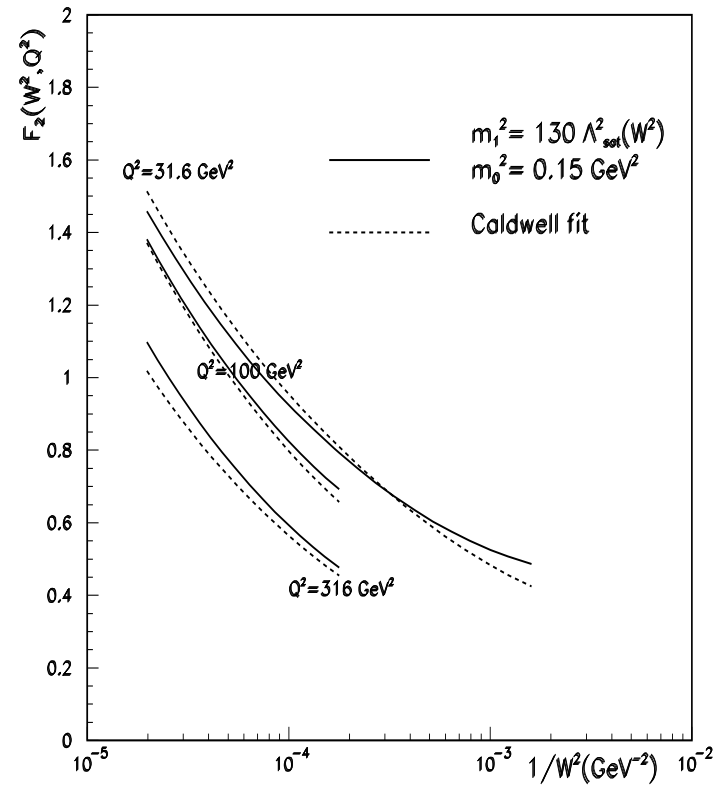
The approach to saturation.

Comparison with Caldwell 6-parameter 2 P-fit: $\sigma_{\gamma^*p} = \sigma_0 \frac{M^2}{Q^2+M^2} \left(\frac{l}{l_0}\right)^{\epsilon_0+(\epsilon_1-\epsilon_0)} \sqrt{\frac{Q^2}{Q^2+\Lambda^2}}$

where

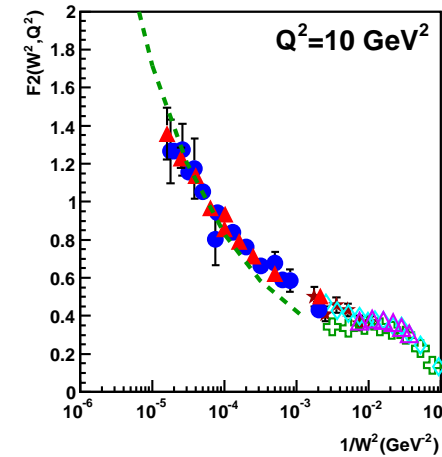
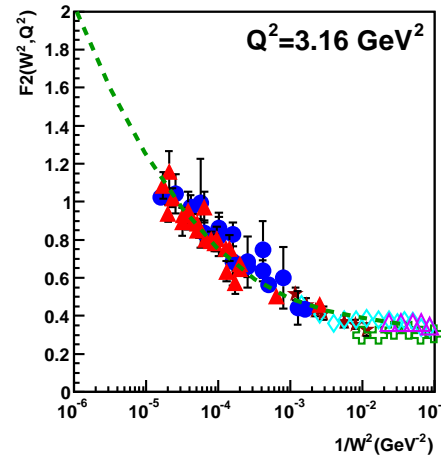
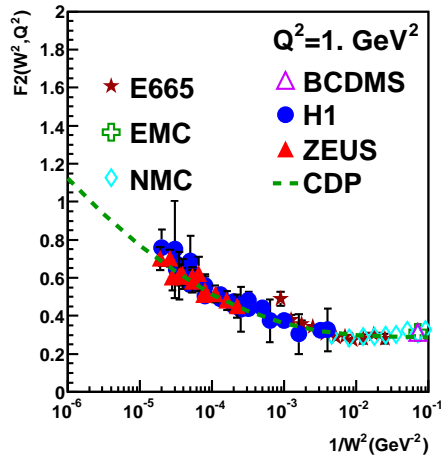
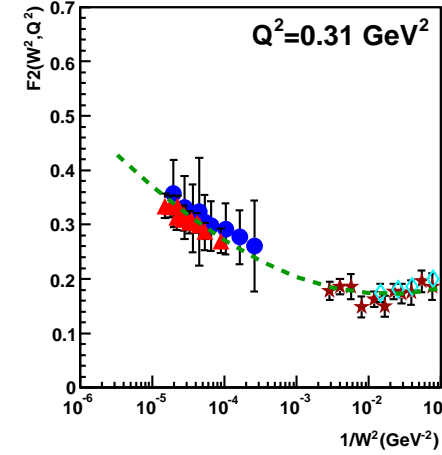
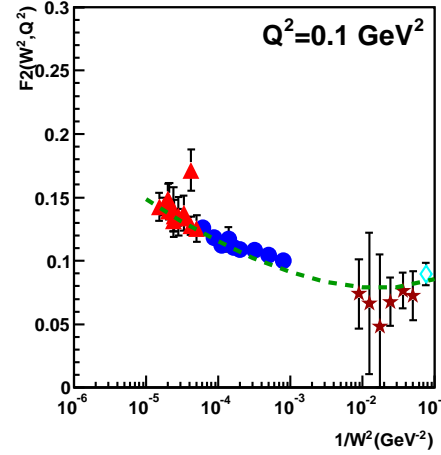
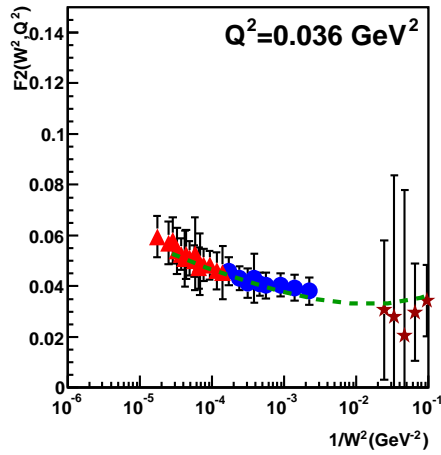
$$l = \frac{1}{2x_{bj}M_p}$$

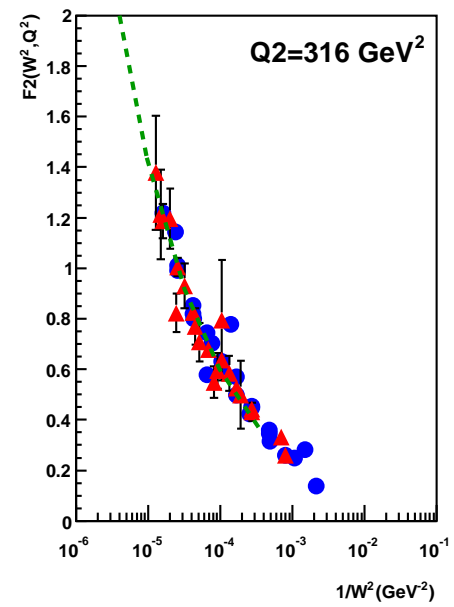
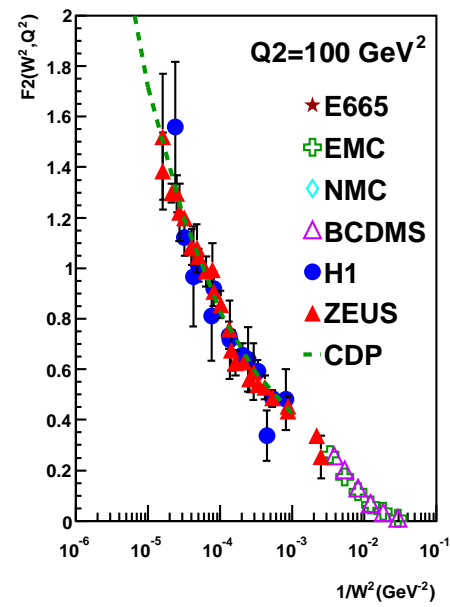
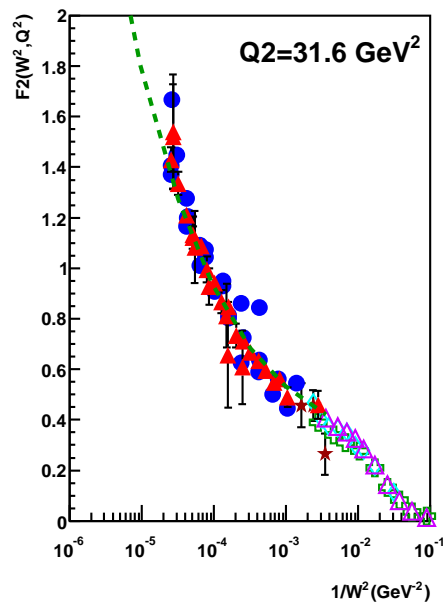




Comparison with the experimental data directly

Prabhdeep Kaur (2010)





Saturation limit: $\lim_{\substack{W^2 \rightarrow \infty \\ Q^2 \text{ fixed}}} \frac{F_2(x \cong Q^2/W^2, Q^2)}{\sigma_{\gamma p}(W^2)} = \frac{Q^2}{4\pi^2\alpha}$

Consider $Q_1^2 = 0.036 \text{ GeV}^2$

and $Q_2^2 = 0.1 \text{ GeV}^2$

$$\begin{aligned} F_2(W^2, Q_2^2 = 0.1 \text{ GeV}^2) &= \frac{Q_2^2}{Q_1^2} F_2(W^2, Q_1^2 = 0.036 \text{ GeV}^2) \\ &= 2.78 F_2(W^2, Q_1^2 = 0.036 \text{ GeV}^2). \end{aligned}$$

$\frac{1}{W^2} [\text{GeV}^{-2}]$	$F_2(W^2, Q_1^2 = 0.036 \text{ GeV}^2)$	$\frac{Q_2^2}{Q_1^2} F_2(W^2, Q_1^2 = 0.036 \text{ GeV}^2)$
$2 \cdot 10^{-5}$	$\cong 0.055$	0.15
10^{-4}	$\cong 0.04$	0.11

$F_2(W^2)$ and gluon distribution.

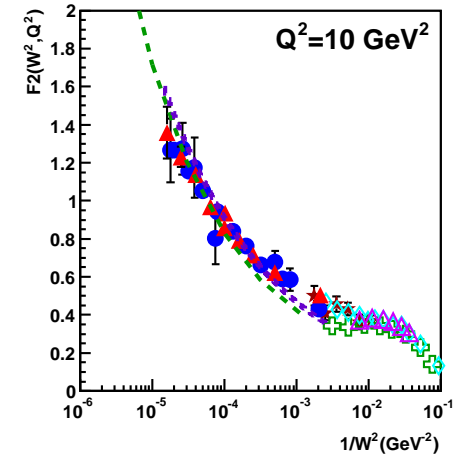
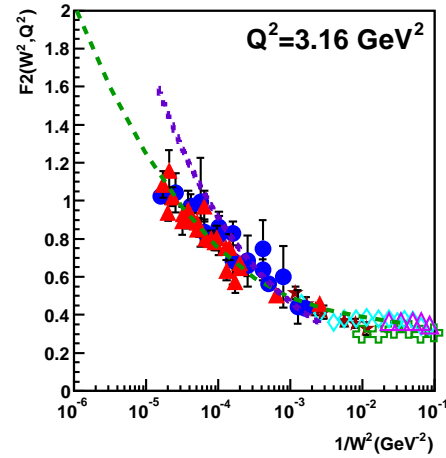
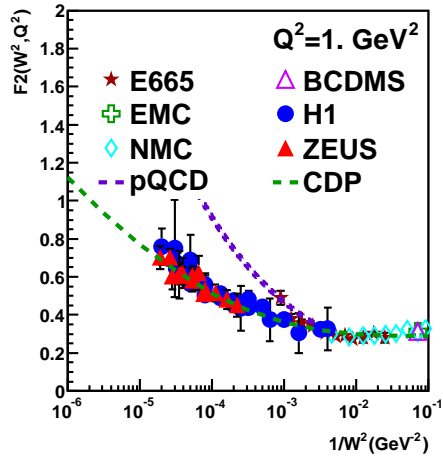
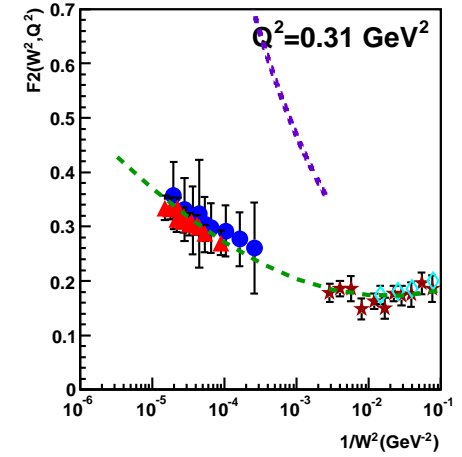
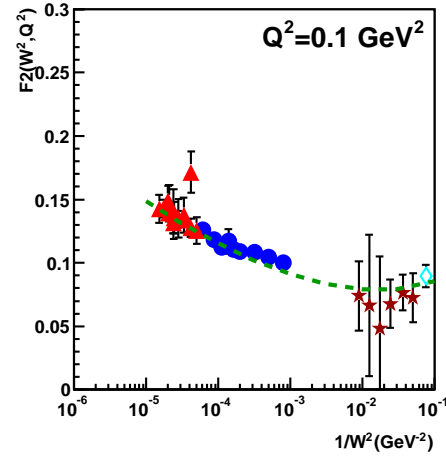
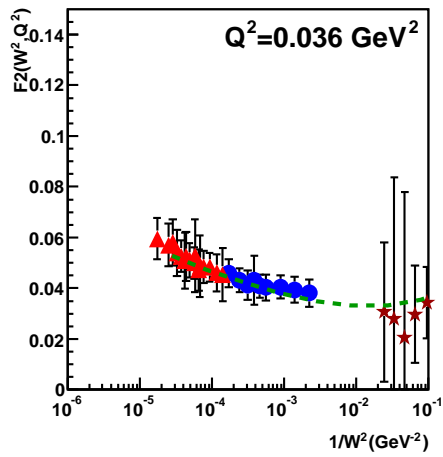
$$F_2(W^2) = f_2 \left(\frac{W^2}{1 \text{ GeV}^2} \right)^{0.29}, \quad f_2 = 0.063$$
$$10 \text{ GeV}^2 \leq Q^2 \leq 100 \text{ GeV}^2$$

In terms of gluon distribution:

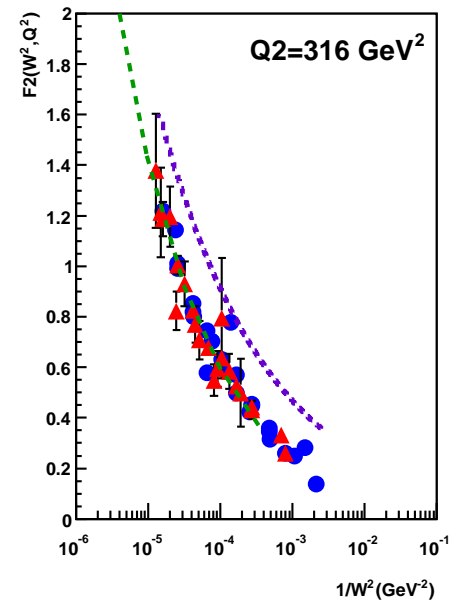
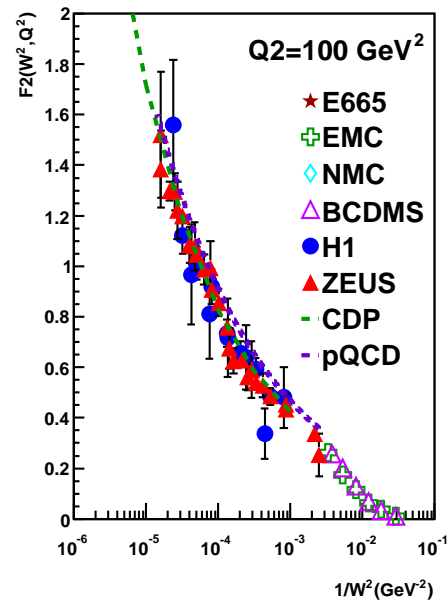
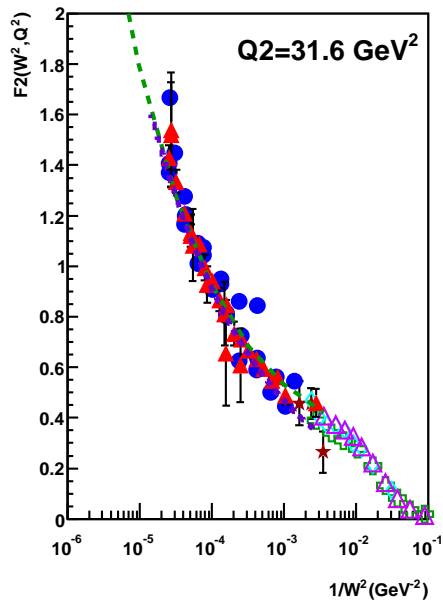
$$F_2(W^2 = \frac{Q^2}{x}) = \frac{(2\rho+1) \sum Q_q^2}{3\pi} \xi_L^{C_2} \alpha_s(Q^2) G(x, Q^2), \quad \eta(W^2, Q^2) \gg 1.$$

Saturation behavior:

$$F_2(W^2, Q^2) \sim Q^2 \sigma_L^{(\infty)} \ln \frac{\Lambda_{\text{sat}}^2(W^2)}{Q^2 + m_0^2}$$
$$\sim Q^2 \sigma_L^{(\infty)} \ln \left(\frac{\alpha_s(Q^2) G(x, Q^2)}{\sigma_L^{(\infty)} (Q^2 + m_0^2)} \right), \quad \eta(W^2, Q^2) \ll 1.$$

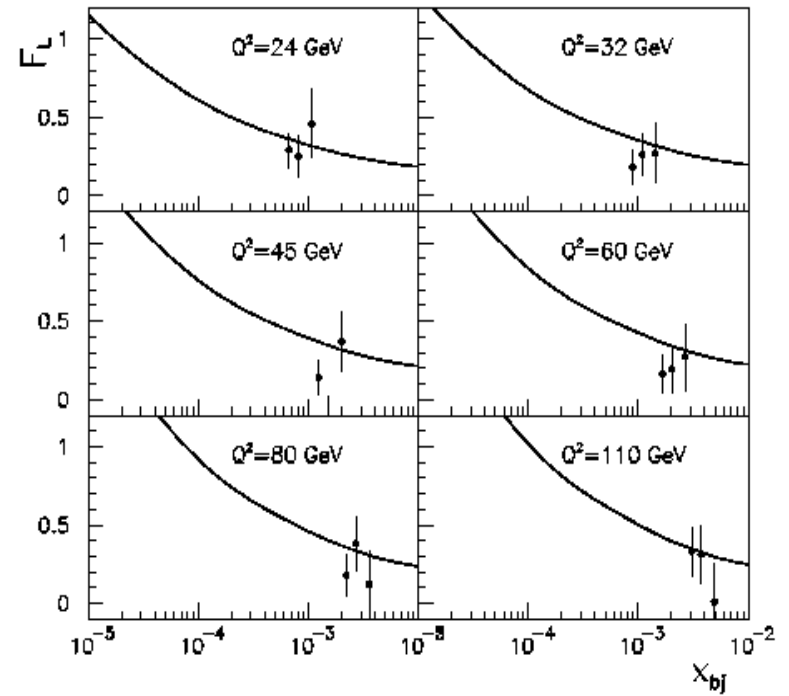
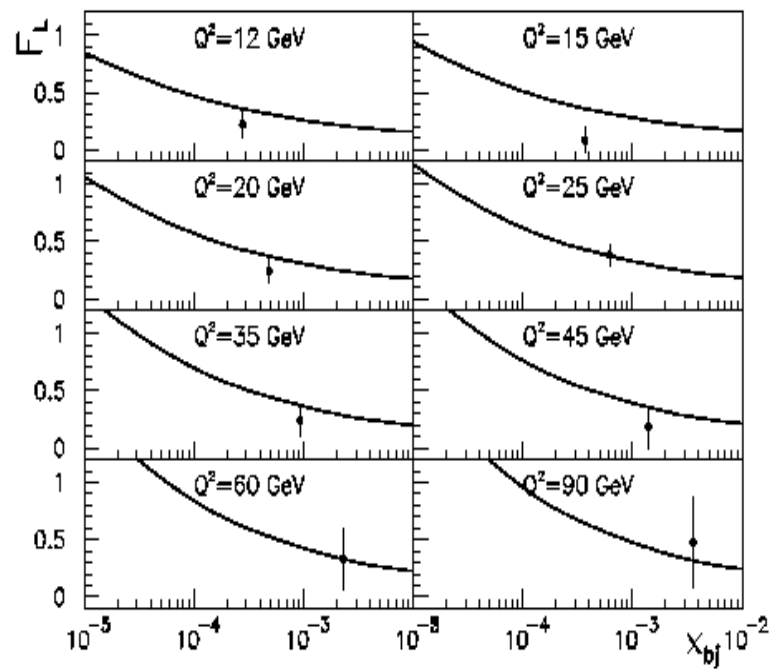


CDP and pQCD-improved parton model



CDP and pQCD-improved parton model

The longitudinal structure function, $F_L(x, Q^2)$



5. Conclusions

Gauge-invariant (two-gluon) interaction of color dipole:

i) Color transparency

$$\sigma_{(q\bar{q})p}(\vec{r}_\perp^2, W^2) \sim \vec{r}_\perp^2, \text{ destructive interference}$$

$$\text{relevant for } \eta(W^2, Q^2) = \frac{Q^2 + m_0^2}{\Lambda_{sat}^2(W^2)} > 1, \quad \Lambda_{sat}^2(W^2) \sim (W^2)^{C_2=0.29}$$

$$\begin{aligned} F_2(x, Q^2) &= F_2(W^2 = Q^2/x) \\ &\sim \Lambda_{sat}^2(W^2), \quad (10\text{GeV}^2, Q^2 < 100\text{GeV}^2) \\ &\sim \alpha_s(Q^2)G(x, Q^2). \end{aligned}$$

Peaceful coexistence between CDP and pQCD-improved parton model

ii) Saturation

$\sigma_{(q\bar{q})p}(\vec{r}'_{\perp}, W^2) \sim \sigma^{(\infty)}$, destructive interference has died out,

relevant for $\eta(W^2, Q^2) < 1$,

$$F_2(x, Q^2) \sim Q^2 \sigma^{(\infty)} \ln \frac{\alpha_s(Q^2) G(x, Q^2)}{\sigma^{(\infty)} (Q^2 + m_0^2)}.$$

Smooth transition from $\eta(W^2, Q^2) \gg 1$ to $\eta(W^2, Q^2) \ll 1$, including $Q^2 = 0$.

There is only a single Pomeron.

Concrete model, interpolating the regions of $\eta(W^2, Q^2) > 1$ and $\eta(W^2, Q^2) < 1$, describes experimental data for $x \lesssim 0.1$, including $Q^2 = 0$ photoproduction.